Projekt zum Fortgeschrittenen-Praktikum - Atomic Force Microscopy

Guilherme Stein & Ulrich Müller

During the AFM experiment we investigated the surface roughness of four GaSb samples. While an untreated GaSb wafer shows ditches caused by polishing the overgrow of a 200 nm GaSb buffer leads to significant lower surface roughness. Two different growth temperatures were tested. The buffer grown at 515° exhibited a lower surface roughness than the one grown at 485°. Furthermore we tested a sample with a 30 nm AlAsSb layer on top of a 170 nm GaSb layer. On the one hand we found even lower average surface roughness. On the other hand single peaks in range from 4 nm to 6 nm were not removed from the surface as it indicated previous publications [4].

Supervisor: Dr. Paolo Sessi

Date of experiment: 4$^{\text{th}}$ October 2013

1. Motivation

The III-V semiconductor system based on GaSb is commonly used for optical semiconductor devices with wavelengths beyond 2.3 µm [1]. In Würzburg especially the interband cascade lasers, which are grown by MBE on GaSb substrate, made significant progress during the last years [2]. In order to grow devices with high performance it is inevitable to use high quality substrates with a minimum of defects. Despite the use of 'epi-ready' substrates the wafers suffer from native oxide like Ga_2O_3 and Sb_2O_3 [3]. The growth of devices on top of this oxide would lead to non-monocrystal layers. To remove this oxide a commonly used technique in Würzburg is to heat the substrate to about 580° for a short time. At this temperature the most of the oxide desorbes from the surface but leaving holes in the surface with about 10 nm in size [4]. Hereupon a 200 nm GaSb buffer layer is grown at 485° to flatten the surface.
This method has been established during the last years although it is not clear whether a different technique would lead to smoother surfaces. Therefore one of the goals of this experiment is to determine a method of reducing the roughness on the wafer we want to grow on optical structures. This is important on the behalf of the optical quality the device can operate at.

From an intuitive point of view it is clear what roughness is. However, quantifying roughness in a mathematical way is not trivial. Common definitions use the standard deviation of the surface's mean height as $S_a = \frac{1}{A}\iint\limits_A |z(x,y)|\mathrm{d}x\mathrm{d}y$ and are suitable in many applications. Problems arise when applying this definition to non-flat surfaces. A soup bowl which appears flat and smooth when we are very close to the surface, shows a curvature when we look at the object as a whole. This example shows, that roughness is not independent of the scale. In our scope roughness will be a way of measuring the quality of a surface with respect to certain properties of the material. We think that in general the concept of a surface energy is a better approach to address the optical properties arising from surface irregularities. The more the size of the surface differs from a perfect flat surface the rougher the surface is. We want to model the surface as polygons connecting the mean heights of a discrete lattice. The lattice size represents the scaling parameter mentioned above. Here we make the arbitrary choice of the AFM's resolution which will be the scale on which we measure the roughness of the samples.

The Atomic Force Microscope (AFM) is the perfect instrument to characterize this roughness of the wafers as it determines the height of the surface very precisely. The expected differences in height on the sur-

Figure 1: At the sample's surface after several micrometer growth small pyramidal defects are visible. The image was taken by an optical microscope at a magnification of 50.

face is about 10 nm which is within the resolution of the AFM. As the AFM doesn't work in situ we have to produce and investigate the surface at each step of the growth process to understand the mechanisms of oxide desorbtion and flattening of the surface. We are going to characterize the single steps of the standard process which are: an untreated GaSb wafer, the wafer after the oxide desorbtion and after the growth of 200 nm GaSb buffer. To vary this process we want to test two aspects: first the increase of the GaSb buffer's growth temperature up to 500° and 515° and second the growth of a 30 nm GaSb/AlAsSb superlattice directly after oxide desorbtion. Recent research showed that the growth of AlAsSb shutting down the step-flow growth mode. This step-flow growth mode is dominant during the growth of GaSb layers and is not very successful in flattening bigger defects like defects in pyramidal shape [4]. The growth of a superlattice instead of a bulk layer is nevertheless necessary to maintain the electrical conductivity of the sample. It would be helpful to understand how these defects can be removed from the surface and how the process can be improved. If the smoothing is not successful theses pyramidal defects tend to grow bigger as the growth progresses. After the growth of structures with a thickness of several microns these defects can even be observed by a optical microscope as shown in figure 1.

After sample production exposure to air can not be avoided. To reduce surface corrosion the samples will be produced tight before the experiment and stored in a nitrogen-flooded cabinet.

2. Basics

The relevance of fabrication and therefore also the analysis of structure in the sub-micrometer and even nanometer scale has increased steadily in the past decades. In contrast to other scanning imaging techniques as the STM or SEM, the atomic force microscope (AFM) is capable to deliver up to atomic resolution without the need of a vacuum or special treatment of the probe prior to analysis. This allows us to examine a broader variety of samples under easily achievable conditions.

2.1. Principle of the AFM

The principle of the atomic force microscope are the forces that act between two pieces of matter when brought close to each other. More precisely we bring a sharp tip into a distance of a few nano meters to a surface of interest. At this scale the main contribution are Van-der-Waals forces which arise from polarisation fluctuations in the material and the repulsive forces due to Fermi's exclusion principle. In figure 2 one can see the main parts required to run the AFM. The sample is mounted on a xyz-stage consisting of different piezo elements. This enables us to move the sample in xy-direction for the scanning of the probe, as well as in the z direction for height compensation. A reflecting cantilever is positioned above the sample. A laser beam reflects on the cantilever and hits a segmented photodiode. If the cantilever moves, the laser beam will change the angle of deflection. From the intensity change on the diode segments the height difference of the material is derrived.

2.2. Technical refinements

Instead of mapping the intensity change on the diode to the force and subsequently to the probe height, often a different approach is used. The tip is set to apply a constant force on the probe. If the force changes, the piezo in z-direction is altered to move the probe to a height where the force is equal to the set point defined before. This has the advantage that the force

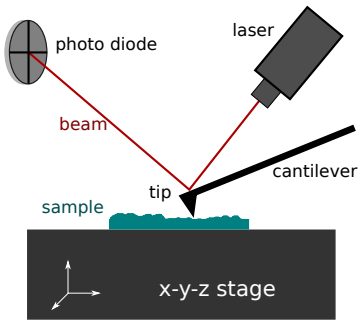

Figure 2: Simplified illustration of an atomic force microscope

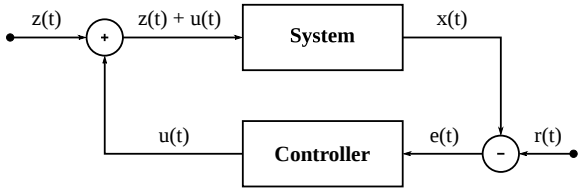

Figure 3: Principle of a feedback loop with characteristic variables: disturbance $z(t)$, set point $r(t)$, control signal $u(t)$, measured output $x(t)$ and error signal $e(t)$.

between tip and probe is approximately constant and therefore it is less likely to damage the sample or the tip. This is ensured via a feedback loop between the the diode and the piezo element as seen in figure 3. The height information accquired via this method is more strongly connected to the actual sample surface. The mapping is done between the piezo voltage as opposed to the strength of the diode, the angle of the laser beam and the distances between those elements. Therefore introducing less error sources and leading to a more accurate signal.

The resolution of the used AFM is within the range of several nanometers. This is adequate to measure the surface of the GaSb-wafers. These samples are normally characterized by optical microscopy, X-ray diffraction and scanning electron microscopy. As these techniques offer very less information about the sample's surface structure the AFM provides us a new possibility to gain this information.

3. The AFM Experiment

3.1. Samples

In section 1 we described different samples of interest. Since we encountered problems during the sample growth, measurements were only performed on four of the samples. The samples are listed with a short description in section 3.1.

sample	property
①	An untreated GaSb wafer
②	200 nm GaSb buffer at 485°
③	200 nm GaSb buffer at 515°
④	10 nmGaSb buffer plus
	30 nm AlAsSb plus
	160 nm GaSb buffer at 515°

3.2. Parameters of recording

In order to acquire the topology of the samples surface the computer records the scanner's z-position in combination with the in plane x- and y-position. These data can be exported from the control software in a special (.ezd) data format. We convert these data back into a list of x, y and z-coordinates using the *WSxM* software, which is freely available on [6].

While scanning in static force mode it is necessary to maintain the force constant by moving the scanner's z-position. This is done via a feedback loop, which compares the set force to the force calculated from the signal of the photodiode. The difference is called the error signal and is the input for the PI-controller. In the AFM control software the **P**(roportional) and **I**(ntegral) parts are adjustable. While recording the data we can adjust the **P** and **I** values to optimize the respose of the feedback loop thus reducing image artifacts. These values refer to the proportional and integral gain of the z-controllers feedback loop respectively. By increasing the **P** value one should observe a smaller static error and a faster adaption to the current height position. On the other hand, if this value is set to high, overshoots while scanning steps are likely. Even higher **P** values lead to more noise as the scanner is reacting oversensitive to little changes in height. The **I** parameter defines the contributes proportional to the time integral of the error signal.

In the beginning of the experiment we scanned a calibration grid while varying the P and I parameter to estimate the effect on the scan and picture quality. The calibration grid consists of a grid with two different height levels. By scanning the grid in one direction one should observe steps in the up and down direction.

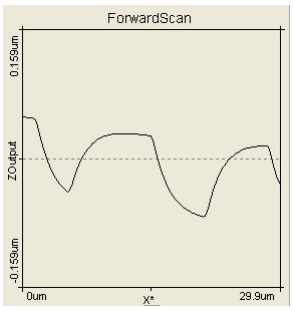

(a) I-gain set to 5. P = 9.

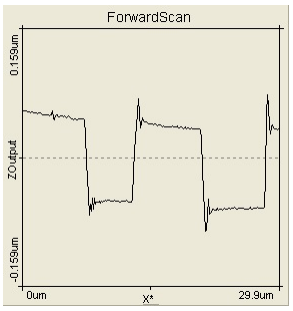

(b) I-gain set to 11. P = 9.

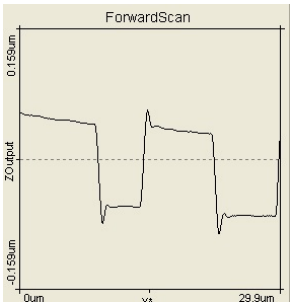

(c) P-gain set to 5. I = 9.

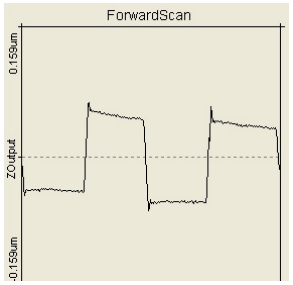

(d) P-gain set to 15. I = 9.

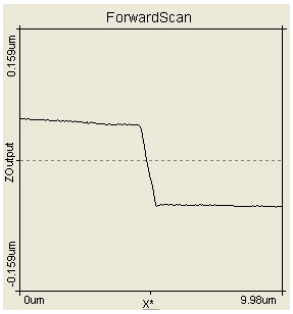

(e) Scanning speed of 3 s per line. P = 9, I = 9.

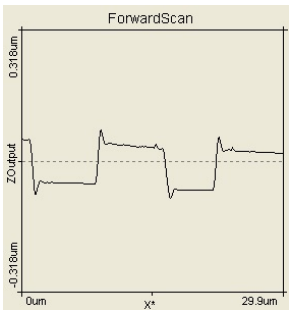

(f) Scanning speed of 0.7 s per line. P = 9, I = 9.

Figure 4: Height profiles of single lines and the effect of different feedback parameters and scanning velocities. Scanning direction is from left to right.

First we started with a low I value and observed the z-coordinate adapting slowly to the actual height of the grid as shown in 4a.

By increasing the I value the height is adapting much quicker but overshoots at the step's edge as well as increasing the amount of noise during the plateaus. The height profile is plotted in 5b.

In the next step the influence of the P value was observed. With the I value set to 9 the P value was varied from 5 to 15. Interestingly a decrease of the P value to 5 does not change much other than increasing the overshoots caused by the I value, which is set little higher than the optimum value. Simultaneously the overshoots decrease when increasing the P-value. This however has a negative influence on the noise shown in the comparison of 4c and 4d.

As a trade-off between fast and accurate height adaption and a minimum of noise we choose I = 9 and I = 7. We use these parameters in all following measurements, if not stated differently.

To investigate what influence the speed of scanning has on the image recording we measure the calibration grid with 0.7 s and 3 s per line. During this period 256 data points are recorded along the scanning axis. At slow scanning speed we observe a clear step of the calibration grid without any noticeable overshoot in 4e. At a faster scanning speed we can see in 4f distinct overshoots at the beginning of each step.

Although we observe artifacts while scanning the calibration grid with 0.7 s per line it is possible to measure smooth structures at higher scanning speeds without observing overshoots.

3.3. Data preparation

When acquiring data there is always an interpretation and processing involved. This is necessary to make sense of the data, especially when dealing with big data sets. This strongly depends on the uses of the data, i.e. getting a general idea of an object or measuring something with great accuracy to search for yet undiscovered principles. While the unprocessed set has little meaning, we edit it and thereby imprint a meaning into the data. Some may argue this leads to wrong data, or at least reduces its quality. On the other hand, there is no such thing as a perfect measurement. Therefore the data we acquire will never be an exact representation of the object we want to project. We need to make corrections based on our model of the world to increase the quality and, even more crucial, the usefullness of our measurements. It is absolutely necessaty not to accidentally manipulate the data in a unscientific manner. Thus we need to know all the time what has been done with the data and to document the process of analysis. With the AFM we scan a sample with great precision in a rasterized format. Each image consists of discrete coordinates. Our goal is to analyse the samples surface. One step is the removal of systematic errors. If the sample is known to be flat we can make a fit to the underground. While manipulating the data quite a bit, we remove a simple error, i.e. a tilt in the plane known

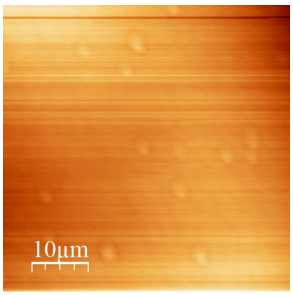

(a) The raw data image from sample ④.

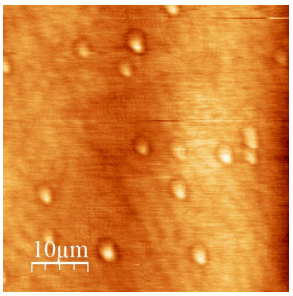

(b) Data of sample ④ flattened in row and column.

Figure 5: Height profiles of single lines and the effect of different feedback parameters and scanning velocities. Scanning direction is from left to right.

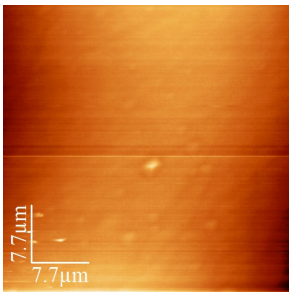

(a) The raw data image from sample ① .

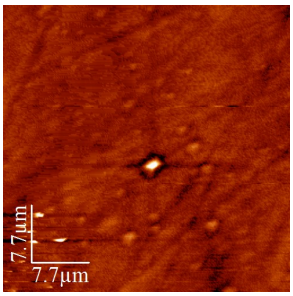

(b) Data of sample ① flattened in row and column. A artifact horizontally and vertically from the peak has emerged.

Figure 6: Height profiles of single lines and the effect of different feedback parameters and scanning velocities. Scanning direction is from left to right.

to be something irrelevant for our purpose. In this case even underground fits of higher order might be useful considering deviations created by nonlinearities of the piezo tube or other elements. On this example we want to show how this is done in detail, when it is legitimate and where problems may occur. In 6a the raw data image from sample ⑦ are plotted.

We can clearly identify the horizontal direction in which the tip scanned the sample. After each row the tip is afflicted with a different offset leading to different heights/colors for each row. This offset is not a feature of our sample, so we try to manipulate the data in a way to get rid of this effect. In detail this is done by fitting a parabola to each row of our sample, subtracting this parabola from the raw data afterwards. The same method applied on the single column removes the tilt in the y-axis. After applying this flatten function the features of our sample are visible much better and the stripy surface has been manly removed.
As mentioned before every correction falsify the data to a certain amount and the method should not be applied without being aware of the problems which may occur.

In the 6a the surface of ① is showed. Noticeable in the middle of the picture we find a peak on a otherwise flat surface. By applying the flatten function we receive the picture shown in 6b. Horizontally and vertically from the peak a darker cross has emerged. This can be explained in the following way. By fitting over the row/column including the peak the mean height is higher. By subtracting the fitted function from raw data, every row/column including the peak is lowered more than the other ones. This leads to an unwanted artifact near the peak.

In summary we consider the flatten method a a legitimate tool for data preparation but one has to be aware of the artifacts which may occur.

3.4. Signal and noise

During the measurements of the calibration grid the amplitudes of the single steps are much higher than the level of noise. While measuring flatter surfaces this in not the case however. During the measurement of sample ④ we observed features which are in order of 4 nm. Here it becomes more and more important to quantify the amount of noise to distinguish between real features and random noise. From the difference between the forward and backward scans we can estimate the amount of noise comprised in our data: First we take the data points from one line, forward and backward, and shift them to a maximum overlap. Secondly we calculate the difference between these two scans. From these aberrations we receive a standard deviation between the two scans. Dividing by $\sqrt{2}$ provides the standard deviation of the measurement. As an example in figure 7 the signal and an area with the size of the measurement's standard deviation is plotted. The signal is calculated by the mean value of the forward and backward scan.

Therefore we can say that the peaks at 100 µm and 185 µm are real features while there is no significance for the peaks beyond 200 µm.

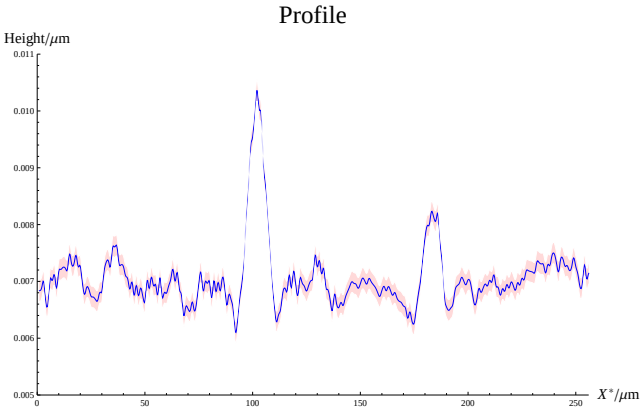

Figure 7: Height profile plotted with an estimation of noise. Two peaks at 100 µm and 185 µm are visible which are much higher than the level of noise.

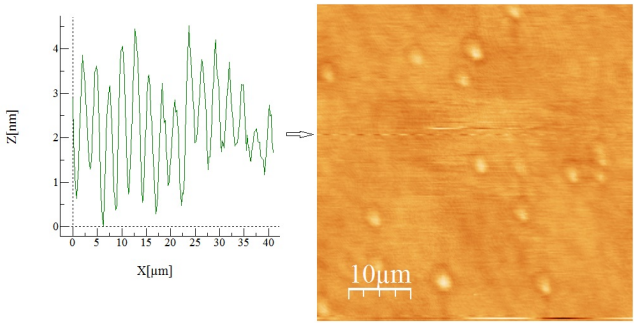

Figure 8: Surface of sample ④. One line recorded a periodic oscillation. This artifart is not visible in the backward scan.

Additionally to the noise we observe artifacts which can be clearly identified as they only appear in one, either forward or backward direction. One artifact we want to discuss is shown in figure 8. In one single line we can see a periodic pattern which is shown in 8. The the periodicity of this artifact is approximately 2.5 µm but we find oscillations with an other periodicity as well. Artifacts on single lines can be caused by small particles which are pushed over the sample by the tip. This however doesn't explain the regular oscillation.

Furthermore we found pattern which looks like concentric sets of ovals. The distance between two ovals decreases as their size increases. We find these elliptic pattern in every of our GaSb samples. One surface with clearly visible patterns is shown in 9. As these pattern are visible in the forward and backward scanning direction they could be caused by features of the surface. On the other hand the ovals don't correlate with the crystal structure or the peaks on the surface which commends

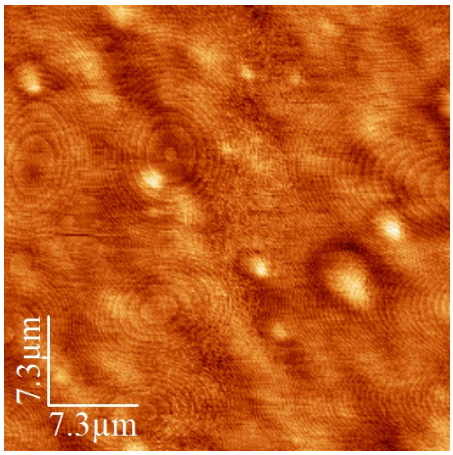

Figure 9: Oval pattern. Sample ④

to an artifact. If it is an artifact it could be on the one hand caused by an interference between a plain and a spherical wave. But to explain the pattern shown in 9 the wavelength should be in the order of 200 nm which is to short for laser light. On the other hand these pattern could be a moiré-pattern caused by the discrete lateral resolution which equals 50 µm/265 = 195 nm.

4. Sample Analysis

On the surfaces of our samples we found single accumulations of material typically in the order of several nanometers. Interestingly in the vicinity of these peaks the average height seems to be significantly lower than on the rest of the surface. It seems like every peak accumulates material from a radius of around 1 µm. This effect can be explained by potentials which cause atoms to move and adsorb at a step while it hinders atoms to leave a plateau. These potentials are calls Schwoebel barriers [5].

As mentioned in section 1 one of the goals of this experiment was to quantify and analyze the roughness ρ of a variety of surfaces. We concluded that an appropriate measure would be the normalized surface area of the interpolated polygons between our background corrected points as measured by the AFM. In principle it denotes the deviation of a flat surface as:

$$\rho = \frac{S_{\text{polygons}} - S_{\text{projected}}}{S_{\text{projected}}} \tag{4.1}$$

For further reference please see appendix A.
To estimate the error of this value we calculate the roughness of a randomly generated surface with a deviation in height which is equal to the noise estimated in 3.4. All the values of surface roughness together with this error are presented in section 4

sample	property	roughness ρ
①	An untreated GaSb wafer	$2.55(7) \cdot 10^{-5}$
②	200 nm GaSb buffer at 485°	$0.61(7) \cdot 10^{-5}$
③	200 nm GaSb buffer at 515°	$0.54(7) \cdot 10^{-5}$
④	10 nmGaSb buffer plus 30 nm AlAsSb plus 160 nm GaSb buffer at 515°	$0.49(7) \cdot 10^{-5}$

In sample ① there are actual scratches on the surface. Since it is the untreated wafer we suspect this arising from a polishment after the fabrication. This sample shows a much larger roughness than the other treated samples. The second sample ② is smooth on most areas, but we find large isolated features across the surface. While the sample ③ is the same as the previous one but grown at a higher temperature, we do not find those larger features on the surface and therefore the surface is even smoother. The smallest roughness was measured on sample ④ . On this sample a layer of AlAsSb was grown, producing a few wider features only little higher than the average. But as the overall surface is smoother, this contribution is not as big as to increase the roughness above the other samples. Here the corrected samples were described. Except for the untreated sample ① the background correction yields a decrease of the roughness of about a factor of two. Although there is a flattening involved in this correction the largest contribution is attributed to the fact that the scan lines are fitted separately. Irregularities and systematic errors arising from the fact of line switching or directional changes are thereby minimized.

5. Summary

During the AFM experiment we investigated the surface if different samples. Starting with a calibration grid we investigated the influence of different scanning parameter like P and I feedback-loop values and different scanning speeds. Furthermore we investigated the roughness of four GaSb samples. While an untreated GaSb-wafer shows ditches caused by polishing the overgrow of 200 nm GaSb buffer leads to significant lower surface roughness. Two different growth temperatures were tested. The buffer grown at 515°exhibited a lower surface roughness than the one grown at 485°. Further we tested a sample with a 30 nm AlAsSb layer during the GaSb layer, which was itself reduced to 170 nm. On the one hand we found even lower average surface roughness. On the other hand we found single peaks in range from 4 nm to 6 nm which were not removed from the surface as it indicated previous publications [4]. Different kinds of artifacts were discussed and we showed the advantages and risks of data preparation.

References

[1] Shamsul Arafin (2012): Electrically-Pumped GaSb-Based Vertical-Cavity Surface-Emitting Lasers. München.

[2] Weih, Robert; Kamp, Martin; Höfling, Sven (2013): Interband cascade lasers with room temperature threshold current densities below 100 A/cm2. In: Appl. Phys. Lett. 102 (23), S. 231123. DOI: 10.1063/1.4811133.

[3] C.J. Vineis; C.A. Wang; K.F. Jensen (2001): In-situ reflectance monitoring of GaSb substrate oxide desorption 2001.

[4] Murray, Lee M.; Yildirim, Asli; Provence, Sydney R.; Norton, Dennis T.; Boggess, Thomas F.; Prineas, John P. (2013): Causes and elimination of pyramidal defects in GaSb-based epitaxial layers. In: J. Vac. Sci. Technol. B 31 (3), S. 03C108. DOI: 10.1116/1.4792515.

[5] J. Merikoski; S.C. Ying (1997): Collective diffusion on a stepped substrate. In: surface science letters.

[6] http://www.nanotec.es/products/wsxm/download.php.

A. Roughness calculation

Here “dat” is a 65536×3 data array consisting of 256 rows of 256 points of a (x,y,z) tupel as coordinates.

```
dmatrix[dat_, rowlength_: 2^8] := Partition[data[dat], rowlength]

surface[dat_, rowlength_: 2^8] :=
    (Ad = 0; Au = 0;
    For[i = 1, i < rowlength,
            For[k = 1, k < rowlength,
        Ad +=
            Norm[(dat[[k]][[i + 1]] - dat[[k]][[i]])\[Cross]
                (dat[[k + 1]][[i]] - dat[[k]][[i]])]/2;
        Au +=
            Norm[(dat[[k]][[i + 1]] - dat[[k + 1]][[i + 1]])\[Cross]
                (dat[[k + 1]][[i]] - dat[[k + 1]][[i + 1]])]/2;
        k += 1];
   i += 1];
   Return[Ad + Au])

rough[dat_] :=
 ScientificForm[
        surface[dmatrix[dat]]/(Last[data[dat]][[1]]*Last[data[dat]][[2]]) -  1
               ]
```

B. Sample table

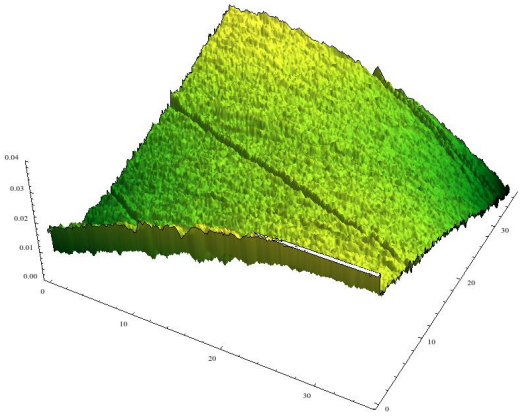

(a) Sample ① : GaSb untreated wafer, original scan. $\rho = 3.62 \cdot 10^{-5}$

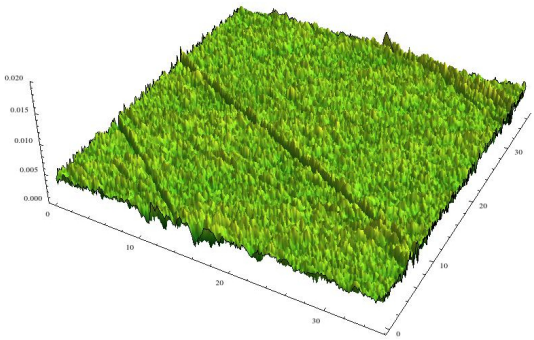

(b) Sample ① : GaSb untreated wafer, fit. $\rho = 2.55 \cdot 10^{-5}$

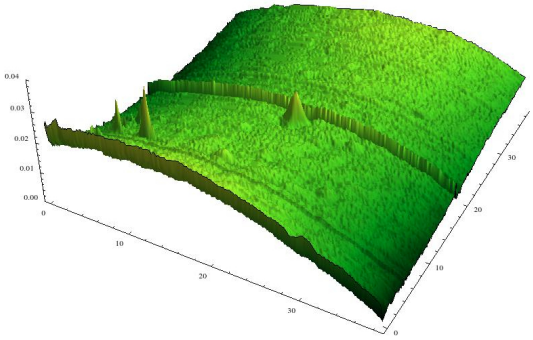

(c) Sample ② : GaSb grown at 485°C, original scan. $\rho = 1.51 \cdot 10^{-5}$

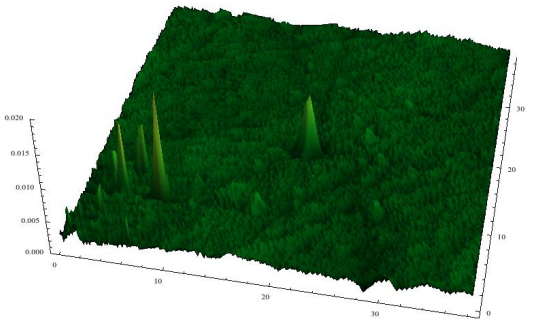

(d) Sample ② : GaSb grown at 485°C, fit. $\rho = 6.08 \cdot 10^{-6}$

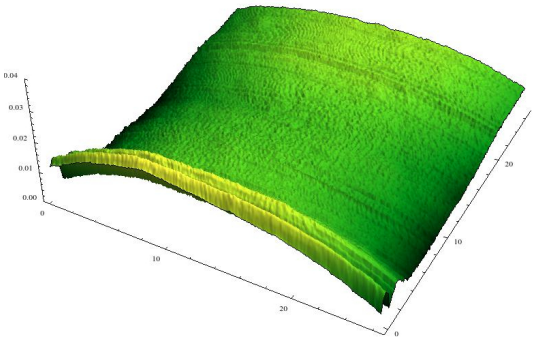

(e) Sample ③ : GaSb grown at 515°C, original scan. $\rho = 1.45 \cdot 10^{-5}$

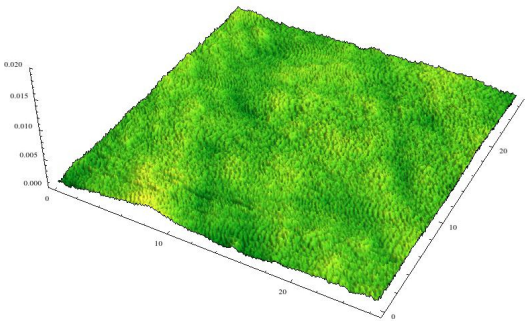

(f) Sample ③ : GaSb grown at 515°C, fit. $\rho = 5.44 \cdot 10^{-6}$

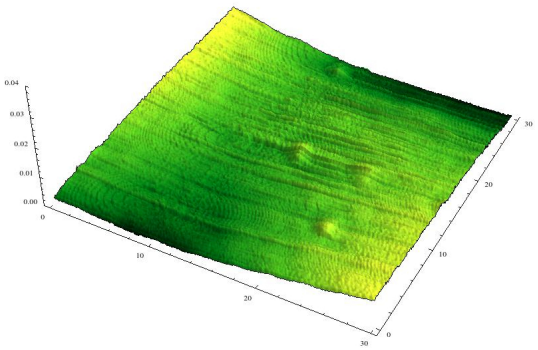

(g) Sample ④ : Al grown on wafer, original scan. $\rho = 1.11 \cdot 10^{-5}$

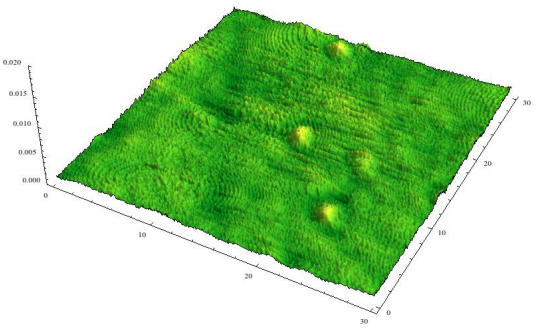

(h) Sample ③ : GaSb untreated wafer, fit. $\rho = 4.85 \cdot 10^{-6}$

Figure 10: On the left the original data is plotted, on the right the data is background corrected by a parabolic fit. ρ is the normalized roughness of the surface as of appendix A